

# NONLINEARITY MITIGATION AND THE SYSTEM CAPACITY ENHANCEMENT OF THE OPTICALLY ROUTED NETWORK (ORNS) BASED ON DIGITAL NONLINEARITY COMPENSATION (NLC) TECHNIQUES

R. Hema<sup>1</sup> and Dr. S. Lakshmi<sup>2</sup>

<sup>1</sup>Associate Professor, <sup>2</sup>Professor,

<sup>1,2</sup>Department of Electronics and Communication Engineering,

<sup>1</sup>Madha Engineering College, <sup>2</sup>Tagore Engineering College, Tamilnadu, India

<sup>1</sup>hema.ebin@gmail.com, <sup>2</sup>drlakshmi79@gmail.com

**Abstract**—In this paper, the non-linearity mitigation of the fully loaded coherent optical networks like Dense Wavelength Division Multiplexing (DWDM) and Coarse Wavelength Division Multiplexing (CWDM) were investigated and experimentally demonstrated. The objective of this optical network is to expand the system capacity in terms of high data rate and bandwidth. However, it has associated with its nonlinear interference noise (NLIN) which degraded the optical system capacity. It is not easy but, achievable by using proper digital Nonlinearity Compensation (NLC) techniques such as Back Propagation (BP) and equalization of nonlinear Phase and Polarization Rotation Noise (PPRN). Such a technique is applied in the above system whose configuration includes a different modulation format from QPSK to 16-QAM with single-carrier and digital subcarrier multiplexed (SCM) optical super-channels through both point-to-point line systems and optically-routed networks (ORNs). The test result conveys that the system gain of the single-carrier has improved by adding more number of BP channels, that is, beyond three joint BP channels; the gain of the NLIN is limited to 0.1 dB after adding per BP channel and also requires PPRN removal at the receiver. However, for a wide range of system configurations, SCM is suitable for the potential benefits of BP and PPRN removal. Here, it has achieved almost similar gain as compared to BP and also PPRN removal is much stronger than BP for higher-order modulation formats which in turn induces high spectral efficiency system. On the whole, the overall context of SCM shows that it not only limits nonlinearity but also induces significantly smaller performance variations in various ORN scenarios.

**Keywords**—Back Propagation (BP), Phase and Polarization Rotation Noise (PPRN) and Digital Subcarrier Multiplexed (SCM).

## I. INTRODUCTION

Nonlinearity mitigation is one of the most important prime factors that required enhancing the system performance of wide range of the optically routed network (ORNs). Nowadays, various methods are involved in overcoming the nonlinear impairments in the Optically Routed Networks (ORNs). It can be induced due to interference which is classified into three types such as (i) signal-signal interference, (ii) signal-noise interference and (iii) noise-noise interference. In the ORNs, the transmitted signals are strongly affected by the co-propagating noises which significantly suppress the portions of the system bandwidth. Therefore, signal-signal interference constitutes the predominant nonlinear effect. Again, it can be further divided into in-band and out-of-band nonlinear interference. In case of in-band, interference combines all type of nonlinearity effects contributed in the bandwidth of the Transmitter (Tx) and Receiver (Rx) to form processed (intra-channel) and additionally included co-processed channels (super-channels) respectively. On the other hand, out-of-band interference generated by ORNs which is inaccessible to both (Tx) and (Rx) and is treated as non-removable noise and later, it has to be defined as Nonlinear Interference Noise (NLIN). In recent years, different digital signal processing (DSP) strategies have been proposed to reduce the nonlinearity effects. Therefore, many researchers are inspired and intensively involved their work to design the digital nonlinearity compensation (NLC) schemes associated with digital signal processing (DSP) algorithms for dispersion uncompensated coherent systems. It can be achieved by proper study about different nonlinear impairments including Self-Phase Modulation (SPM), Cross-Phase

Modulation (XPM), Four-Wave Mixing (FWM), Phase and Polarization Rotation Noise (PPRN). The nonlinear interaction between the ESE of interest and a single interfering ESE (either in-band or out-of-band) is referred as Cross-Phase Modulation (XPM). Similarly, the nonlinear interaction between more than a single interfering ESE (either in-band or out-of-band) is referred as Four-Wave Mixing (FWM). Fig. 1 and Fig. 2 represent the range of Elementary Spectral Entity (ESE) generated by its own optical modulator and types of nonlinearities within a WDM system respectively. It can be grouped together for digital co-processing using NLC algorithms. In this paper, various nonlinear impairments are reviewed and tested under different system configurations such as higher order modulation formats from QPSK to 256-ary QAM with single-carrier and digital subcarrier multiplexed (SCM) optical super-channels through optically-routed network (DWDM & CWDM). From the study [10] explore the potential merits and demerits of digital back-propagation (BP) and the approach reduces the nonlinear interference noise (NLIN) by equalizing the nonlinear form of phase and polarization-rotation noise (PPRN). Such techniques are recently implemented in the ORNs to get promising solution in the aspects of system capacity and their nonlinear mitigation benefits in the wide range system configuration. Then, to evaluate the NLC benefit in terms of the improvement in the peak signal-to-noise ratio (SNR) with full channel loading across the C-band and considering various higher order modulation formats. The rest of the paper has organized as follows. Section II deals with the potential benefits of both back propagation and digital subcarrier multiplexing. The mathematical model the optically routed network to analysis the system performance through the Peak-Signal to Noise Gain is detailed given in Section III. In section IV, the simulation results of the back propagation and equalization of nonlinear Phase and Polarization Rotation Noise of the optically routed network (ORNs) of the digital subcarriers systems are shown. Finally, the conclusion has been made from the simulation result.

### Overview of Related work:

In this section, the review of various nonlinear impairments are analyzed in the fully loaded coherent optical network likes Dense Wavelength Division Multiplexing (DWDM) and Coarse Wavelength Division Multiplexing (CWDM) systems as well as key Digital Signal Processing (DSP) schemes for their mitigation. J. M. Kahn et all explore the theoretical limits of digital back-propagation (BP) [3] in the single channel optical network and described the mathematical model of two promising Nonlinear Compensation (NLC) techniques [4] to mitigate the nonlinear contributions in the form of phase and polarization-rotation noise (PPRN). According to this, equalization of nonlinear PPRN mitigation has performed based on knowledge of

the phase coherent carriers. Due to lack of phase coherence, the efficiency of the respective DSP algorithms is reduced which in turn affects the system capacity of the ORNs. Joint digital BP [12]–[19] and along with the NLFT [38]–[43] have investigated the In-band nonlinear interference. Then, equalization techniques [20]–[23] mitigate out-of-band XPM contributions which manifest themselves as time-varying Inter Symbol Interference (ISI). Such techniques have been shown to efficiently mitigate mainly the zeroth-order XPM contribution. When it has extended to Higher-order XPM contributions typically exhibit shorter temporal correlations that make their mitigation using adaptive equalization less efficient. Maximum a posteriori (MAP) decoding or maximum likelihood (ML) decoding [24]–[27] enhance the receiver’s performance by taking into account the noise statistics and correlations induced by the ISI form of XPM. It has more expensive in terms of computational complexity and are typically limited to account for only a few ISI contributions. In-band interference, as well as FWM contributions generated by nonlinear interactions between in-band and out-of-band super-channel tributaries or electronic subcarriers, may be partially mitigated as well using equalization techniques, or through MAP or ML decoding. Then, it is extended to digital subcarrier multiplexed (SCM) technique that has recently attracted significant attention with respect to nonlinearity suppression [28]. Based on this, optimizing the subcarrier bandwidth (or symbol rate) is of interest [29]–[30].

## II. BENEFITS OF DIGITAL BACK PROPAGATION

Nonlinearity due to in-band interference can be compensated using appreciate algorithm (Back Propagation) has been implemented at respective transmitter or receiver. The split-step processing and perturbation based approach are most widely used in BP to address the in-band interference in the time domain and frequency domain respectively. However, there occurred high computational complexity while adding number of back propagation channels. To overcome this issue, BP can be modified into different modulation formats, including a minimum number of back propagation channels such as weighted BP, filtered BP, multiplier free BF and multi-stage BP. These BPs have the advantage of lower complexity variants due to a minimum number of nonlinear terms in the computation and also combines the benefits of both split-step processing and perturbation based approaches. However, Polarization Mode Dispersion (PMD) is another impairment which reduces the accuracy of BP due to large number of even and odd channel sets. It can be rectified by using digital BP which can be found on the achievable gains for DWDM and CWDM systems with full channel loading across the C-band with and without SCM operating in an ORN environment.

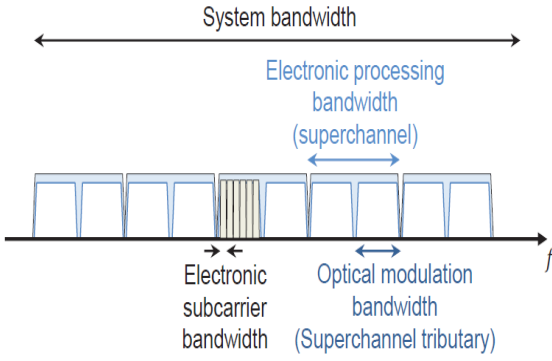


Fig. 1 Set of channels defined in the WDM system

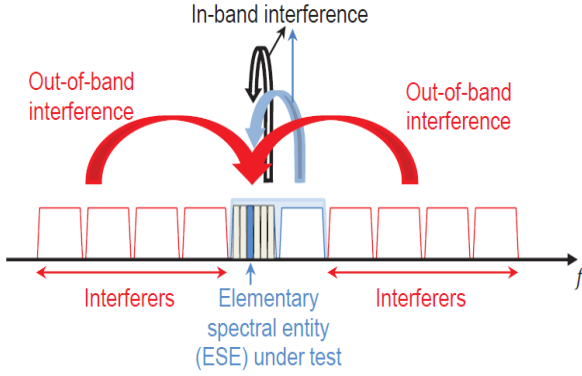


Fig. 2 Types of nonlinearities in the WDM

### A. Systems without Digital Subcarrier Multiplexing:

In this section, the in-band and out-of-band interference of the single-carrier modulated systems have been discussed using an ideal digital BP. The nonlinear mitigation of the single-carrier modulated systems is evaluated with the help of peak-SNR gains through specified system parameters. Firstly, the peak-SNR gain is estimated for in-band interference mitigation by using single channel and multi-channel BP. In this case, the in-band interference can be perfectly removed from  $N-1$  channels of both intra-channel and inter-channel and remaining channels are left with out-of-band interference. In Fig. 3 shows the characteristic of the nonlinear coefficient (dB) with respect to number of back propagation channels for 16-QAM and QPSK transmitter over and respectively. The receiver constellation diagram of the QPSK is well aligned with theoretical predictions but 16-QAM has noise cloud nonlinearity due to non-Gaussian phase variation which is indicated in the form of elliptical portion in Fig. 4. Nonlinear coefficient of the 16-QAM system is about 5 dB which is lower than 16-QPSK system, if the number of channels is jointly processed; which reflects the same amount of peak-SNR gain potential for both systems. However, it shows that peak-SNR gain is very much dependent upon the system bandwidth. The result conveys the significance of signal to signal distortion that is compensated and unavoidable nonlinearity which is induced by amplifier noise. This will affect the high accuracy region gain of the signal to signal. That is, nearly out of 5 channels 2 to 3 channels carry nonlinear

coefficient and similarly, 21 channels and 115 channels case, approximately 14 to 70 channels are affected by nonlinearities due to the propagation of noise. On the whole, in the fully loaded system, nearly around 2/3 of the channels are involved in the noise induction. It is noted that the BP gain achieved from simulation is always smaller than the theoretical prediction. Because of nonlinearities induced from amplifier noise which degrades the potential benefits of BP. Here, equal and average launch power is assumed for all optical channels in which best performance of the center channel is indicated using solid line and worst-performing channel using dashed line. In order to address this issue, the individual BP gain is examined under a fully loaded 115 channels with equal optimized optical power for best performance of the system. For single channel BP, the peak-SNR gain is almost constant around center channels and only few edge channels receive interference. For multi-channel BP, the favorable peak-SNR gains are obtained by perfect removal of the in-band interference and make the edge channels within super channels. For 3-channel BP and 5-channel BP, the peak-SNR gain difference between the center channel and edge channels is only 0.15 dB and 0.25 dB respectively. For 21-channel BP, the difference grows to about 1.2 dB and 0.7 dB. The launched power is optimized for the center channel and edge channel respectively. When, it extend to the super channels, the peak-SNR gain is reduce approximately 0.1 dB lower than center channel due to addition of more and more channels involved in the multi-channel BP. As a result, the actual performance of NLC will be less than the theoretical prediction.

### B. System with nonlinear PPRN mitigation:

In this section, the ways of PPRN contribution analyze and also evaluate the significance of potential gain reduction in the inter-channel. In the Fig. 5 (a) and (b) the overall nonlinear coefficient is breakdown into PPRN (dash-dotted) and non-PPRN (dashed) in systems with single channel BP respectively. It is proof in which the theoretical predictions (lines) exactly matched simulated result (markers). It has obtained by applying before and after PPRN removal using an averaging window of 41 symbols. This will induce perfect PPRN removal and obtained proper peak-SNR gain for 115 channel system employing single-channel BP. In case of 16-QAM, nonlinear PPRN mitigation has quite unavoidable due to constant amplitude formats than QPSK. Due to polarization crosstalk, more predominant contribution of PPRN produces noisy constellation without PPRN removal, where the influence of phase-noise is much more clearly visible for 16-QAM than for QPSK. According to the pulse collision theory, the PPRN becomes more significant when different channel pulses collide in the channel center than at the end of the channel propagation path. That is, length of the propagation path increases simultaneously with the

width of the pulse which will form more incomplete collisions and thus, significantly induce the PPRN. Otherwise, if two far away channel's pulses collide completely, then, PPRN contribution is more in the adjacent channels. Hence, it shows that the significance of PPRN and the gain resulting from its removal increases with system bandwidth and decreases with the length of the link. As a result, the peak-SNR gain is relatively large for short links as compared to long links. However, effective PPRN removal is achievable by doing temporal correlations (efficient equalization) among the collided pulse from far away channels. Hence, it can be examined using the PPRN removal in fully loaded 115 channels system along with and without single channel BP consideration.

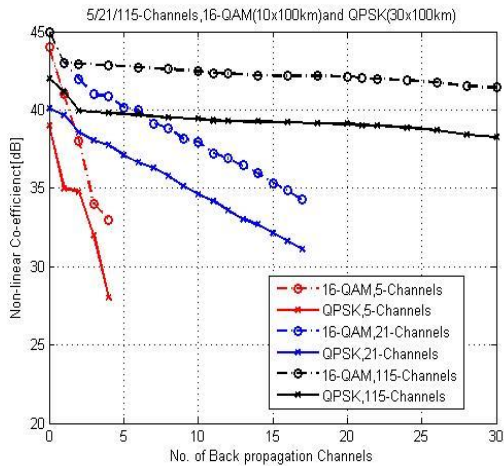


Fig. 3 Nonlinear coefficient versus number of back propagation channels

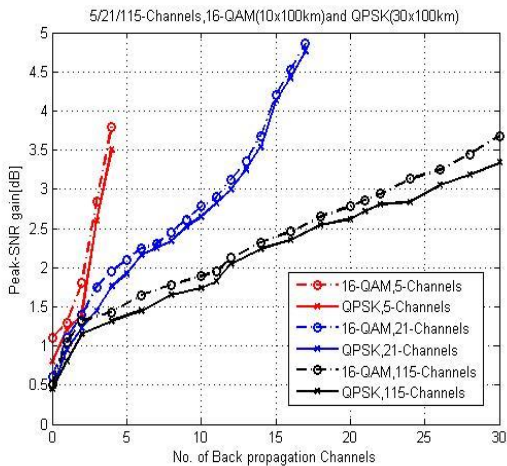
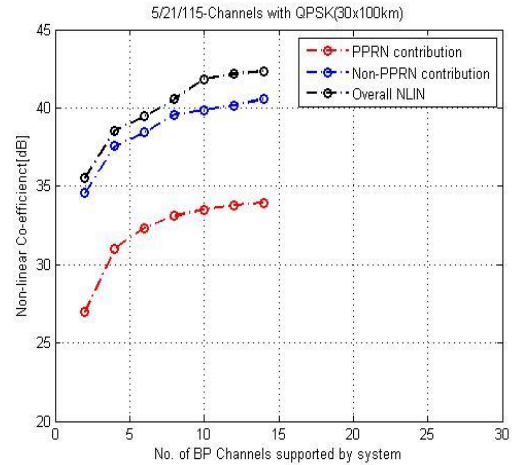


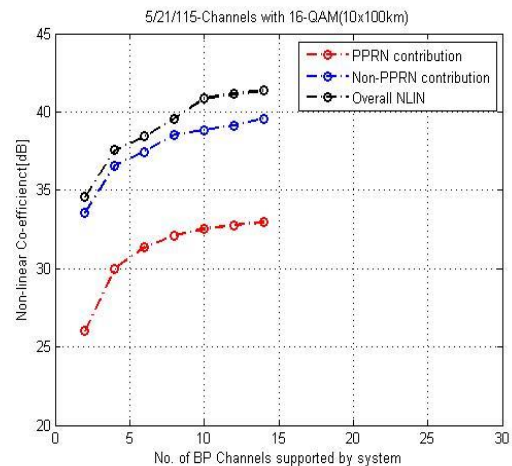
Fig. 4 Peak-SNR versus number of back propagation channels (5, 21 and 115) for higher QPSK and 16-QAM

In the Fig. 6 and 7, it is noted that the PPRN mitigation may be slightly higher for system without single-channel BP than the system with single-channel BP. This is due to the removal of inter-channel PPRN, ignoring other interference from the intra channel, which contributes phase-rotation and polarization coupling. The gain obtained from intra-channel PPRN removal is bounded about 0.5 dB which is similar to perfect single-

channel BP in fully loaded systems. Since intra-channel PPRN removal cannot be better solution to achieve the desired gain than full digital BP, and since the gain of single-channel BP is no more than  $\sim 0.5$  dB in fully loaded WDM systems. This might suggest that PPRN mitigation is more effective and obtain achievable gain for shorter links even in the absence of single-channel BP. In order to enhance the nonlinear PPRN contributions for long links, by considering large number of back-propagated channel which in-turn significantly increases the relative importance of intra-channel nonlinearities.



(a)



(b)

Fig. 5 (a), (b) Breakdown of the nonlinear coefficient into its PPRN (dash-dotted) and non-PPRN (dashed) contributions

However, the achievable gain does not differ from their values in systems without nonlinear PPRN removal. In Fig.8 shows the Peak-SNR gain obtained from perfect inter-channel PPRN mitigation in fully loaded systems with 115 channels without single channel BP of higher order QPSK and 16-QAM respectively. It is observed that the incremental BP gain is slightly higher for 16-QAM and QPSK systems operating over  $10 \times 100$ -km and  $30 \times 100$ -km links, respectively. The gain of single-channel BP is about 0.6 dB whereas the additional gain provided by back-

propagating the two nearest channels is limited to  $\sim 0.3$  dB per channel. The additional gain provided by increasing the number of jointly back-propagated channels beyond three is limited to  $\sim 0.2$  dB for each additional channel.

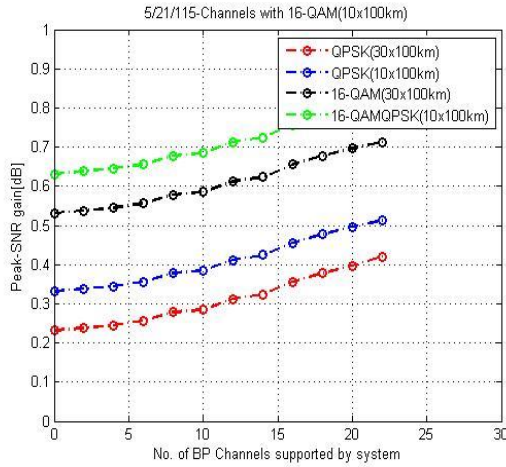


Fig. 6 Peak-SNR gain resulting from perfect PPRN removal, with function of the number of channels.

### III. THE PEAK-SNR GAIN MEASUREMENT

The system performance evaluation is carried out by measuring the peak-SNR gain of nonlinear mitigation under system parameter assumptions at the respectively optimum launch power which is mentioned in Table.1. The signal to noise ratio and interference ratio are involved in the potential gain measurement which is together known as SNIR. In this paper, SNIR is normally referred as SNR which includes both noise and interference. Here, the peak-SNR gain can be considered as the system performance evaluation parameter because it takes only the variance calculation of interference noise and will provide better tradeoff between various basic nonlinear systems. The Fig. 5 shows the allowable peak-SNR gain for various NLC techniques at the optimum signal launch power at each optical amplifier.

Table: 1 System simulation parameters

| Parameters                 | Value                         |
|----------------------------|-------------------------------|
| Channel symbol rate        | 32 Gbaud                      |
| Channel spacing            | 37.5 GHz                      |
| Pulse shape                | SRRC                          |
| Roll off factor            | 0.1                           |
| Span length                | 100 km                        |
| Dispersion                 | 15 ps / (nm - km)             |
| Nonlinear refractive index | $2.6 \times 10^{-20} m^2 / W$ |
| Effective area             | $80 \mu m^2$                  |
| PMD                        | $0 ps / \sqrt{km}$            |
| Loss coefficient           | 0.2 dB / km                   |
| Amplification type         | EDFA                          |

On the other hand, Bit Error Ratio (BER) is considered as an evaluation parameter and is included

before or after a specific forward error correction decoding (pre-FEC or post-FEC BER) is performed. The variance based peak-SNR analysis does not require any assumptions on the probability density of the NLIN. The most accurate prediction can be obtained from the peak-SNR gain by treating the NLIN as additive white Gaussian noise (AWGN) for the system performance measurement. The simulation parameter provides reasonably accurate results in terms of predicting maximum system reach at a given pre-FEC BER. According to NLC methods, more accurate predictions of peak-SNR gain is achieved by taking correlations between the two orthogonal NLIN polarizations which will provide mutual information. The pre-FEC BER prediction is improved by measuring accurate value of peak-SNR gain. The time-domain model of SNR can be written as

$$SNR = \frac{P}{\sigma_{Opt\_Power}^2 + \sigma_{NL}^2} \quad (1)$$

Where  $\sigma_{Opt\_Power}^2$  be the variance of the noise and  $\sigma_{NL}^2$  be the NLIN variance at each optical amplifier respectively. The first-order perturbation approximation is given by

$$\sigma_{NL}^2 = P^3 \chi \quad (2)$$

Where,  $P$  be the average launch power at each optical amplifier and  $\chi$  be the nonlinear coefficient. The different channel's power is calculated from average launched power at each amplifier which will give the approximate nonlinear coefficient value. However, an optimization is relatively low whenever a large number of back propagation channel is added and reasonable channel spacing is maintained. It can be obtained by using Eq. (1) and (2) which will produce the well-known curves characterizing the SNR performance of DWDM systems.

$$peak\_SNR = \left( \sigma_{Opt\_Power}^2 / 2 \right)^{-2/3} \chi^{-1/3} / 3 \quad (3)$$

The NLC methods are used to reduce the nonlinear coefficient  $\chi$ , thus increases the peak-SNR gain is given by

$$peak\_to\_SNR\_gain = \left( \frac{\chi}{\chi_{NLC}} \right)^{1/3} \quad (4)$$

While solving Eq. (4) will give 1/3 dB of improvement in the peak-SNR, irrespective of the noise variance  $\sigma_{Opt\_Power}^2$  by reducing each dB in the variance of NLIN amounts. Based on this, examine the peak-SNR gain by extracting the corresponding nonlinear coefficients  $\chi$  and  $\chi_{NLC}$  from the NLIN Wizard. Hence, it can achieve reasonable improvement in the peak-SNR gain by considering AWGN assumption under certain NLC scheme. According to this, nonlinear interference

noise NLIN variances grow linearly with the length of the link (i.e., a peak-SNR gain of 0.5 dB corresponds to a reach increase of  $\sim 12\%$ ). This will convey that excellent agreement of the overall NLIN variance is similar to the predictions of the enhanced Gaussian noise (EGN) model. The peak-SNR gain is evaluated under perfect nonlinear mitigation (either ideal digital BP or perfect removal of nonlinear PPRN).

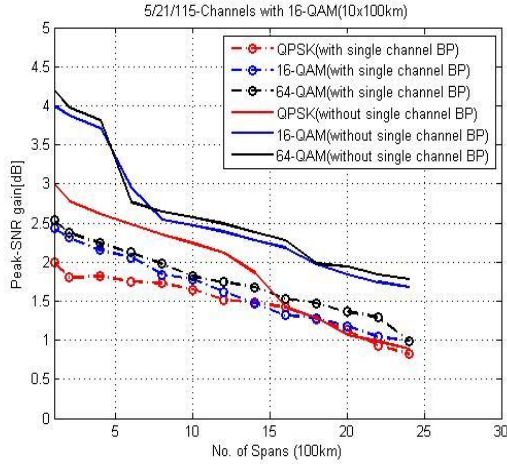


Fig. 7 Peak-SNR gain obtained after perfect inter-channel PPRN removal in fully loaded systems with 115 channels.

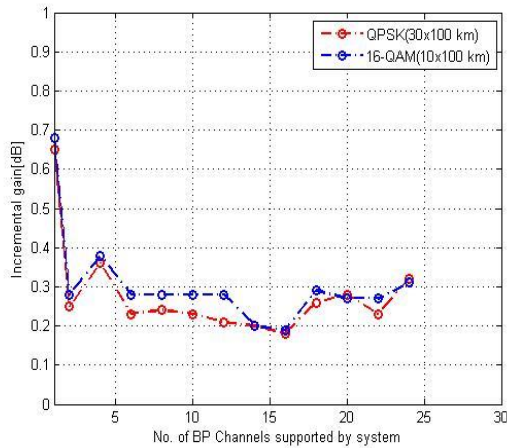


Fig. 8 Peak-SNR gain obtained from perfect inter-channel PPRN mitigation in fully loaded systems with 115 channels without single channel BP of higher order QPSK and 16-QAM respectively.

#### IV. SYSTEMS WITH DIGITAL SUBCARRIER MULTIPLEXING

The nonlinear interference noise suppressed the benefits of the Digital SCM in terms of system performance parameters which includes peak-SNR gain with respect to number of spans respectively. This kind of issues is regained by using the symbol rate optimization where NLIN variance depends on the symbol rate. It can be obtained through Gaussian modulation and phase noise cancellation. According to this, the symbol rate optimization can be significant for QPSK, but rather small for 16-QAM. Later, the

predictions can be expanded including BP and nonlinear PPRN mitigation in systems employing SCM.

#### A. Potential benefit of subcarrier multiplexing:

The available system channels are divided into  $M$  number of statistically independent subcarriers. Here, the number of channels stands for the number of optical channels in which SCM can be performed. For example, a system consists of 21 channels corresponds to 21 optical channels, hence, overall number of subcarriers required is  $21M$ . The potential benefits of subcarrier multiplexing has been estimated by assuming the roll-off factor of 0.1 for the SRRC shaped electronic subcarriers and also considering center subcarrier of the center channel within the system as our ESE under test. Hence, it will conclude the performance of the various subcarriers which is replica of the massive WDM scenarios. The average power is represented as across all subcarriers, where denoting the average launch power of a single optically modulated channel and variance is given as  $(P/M)^3 \chi^{(M)}$ , where  $\chi^{(M)}$  denotes the nonlinear coefficient of the center subcarrier. Therefore, the SNR of the center subcarrier can be written as

$$SNR = \frac{P}{\sigma_{ASE}^2 + P^3 \chi^{(M)} / M^2} \quad (5)$$

In addition, the ASE noise variance for the various subcarriers is given by  $\sigma_{ASE}^2 / M$ , where  $\sigma_{ASE}^2$  representing the ASE noise variance within the entire optical channel. The optimized peak-SNR over  $P$  reveals is equal to  $(\sigma_{ASE}^2 / 2)^{-2/3} (\chi^{(M)} / M^2)$  and the peak-SNR gain resulting from digital SCM is given by

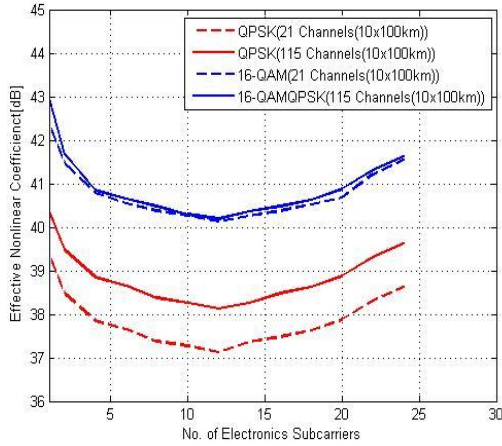
$$\text{Peak-SNR gain of SCM} = \left( \frac{\chi^{(1)}}{\chi^{(M)} / M^2} \right)^{1/3} \quad (6)$$

If  $\chi^{(1)} = \chi$  denotes the nonlinear coefficient in systems without digital SCM, as studied in previous section. Equation (9) shows that the peak-SNR benefit of digital SCM is captured by

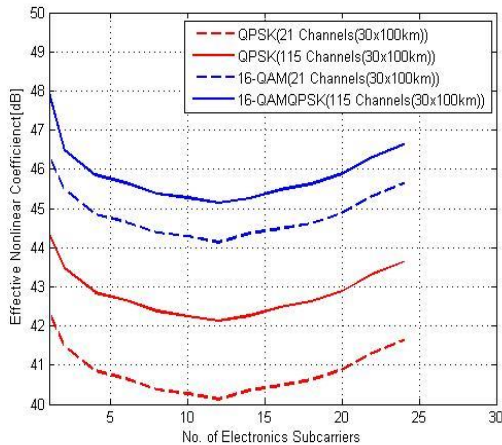
$$\text{Effective nonlinear coefficient} = \frac{\chi^{(M)}}{M^2} \quad (7)$$

The effective nonlinear coefficient in 21- and 115-channel systems is examined in Fig. 15a and 15b where, lines show the theoretical predictions extracted from the NLIN. The maximum deviation between theory and simulation is 0.25 dB in the nonlinear coefficient, which translates into less than 0.1 dB for the peak-SNR gain. The effective nonlinear coefficient exhibits a convex shape with a minimum at 7 and 12 subcarriers for 1000-km and 3000-km systems, respectively. At this optimal number of subcarriers, the reduction of the nonlinear coefficient with respect to single-carrier transmission is about 2 dB for QPSK and 1 dB for 16-QAM. In Fig 9 (a) and 9 (b) circles indicating the effective nonlinear

coefficient extracted from split-step simulations, considering 10-span systems using 16-QAM (red circles) and 30-span systems using QPSK (blue circles). In Fig. 15c examined the effective nonlinear coefficient of the various electronic subcarriers under a fully loaded 115-channel optical system. With respect to single-carrier transmission, the center subcarrier gains the least as compared to the edge subcarriers gain due to insertion of the guard band between the optically generated channels. The performance difference is restricted within  $\sim 0.6$  dB in terms of the nonlinear coefficient.



(a)



(b)

Fig. 9 (a), (b) shows the effective nonlinear coefficient of the 10 and 30-span systems as a function of the number of subcarriers  $M$

The number of subcarriers from  $M = 1$  to  $M = 16$  has represented in various curves in the above mention graph. For sufficiently short links, the peak-SNR gain of a given subcarriers is equal to zero, which means the single-carrier transmission is superior. Thus, the benefit of SCM increases when the number of spans increases and again come to down after reaching a maximum with respect to the link length. The solid black curves show the maximum peak-SNR gain that can be achieved with digital SCM. According to this, beyond 10 spans, the

maximum gain is between 0.6 dB and 0.8 dB for QPSK and between 0.3 dB and 0.45 dB for 16-QAM respectively. The optimal number of subcarriers is plotted with respect to the number of spans which is given in Fig. 16c. The dash-dotted curve shows theoretical predictions for the optimal number of subcarriers, given by  $B/B_{opt}$  where  $B$  is the bandwidth of the individual optical channel and  $B_{opt}$  is the optimal subcarrier bandwidth (or the optimal subcarrier symbol rate)

$$B_{opt} = \frac{B}{\sqrt{\pi |\beta''| LB (\Omega - B/2)}} \quad (8)$$

Where  $\Omega$ ,  $L$ , and  $\beta''$  being the channel spacing ( $= 37.5$  GHz in our case), link length and dispersion coefficient of the fiber. The optimal number of subcarriers is shown to follow the theoretical predictions quite accurately.

## B. Reasons for the SCM performance gains:

In this subsection, the reasons for the dependence of NLIN on the number of subcarriers have been discussed. In the study of SPM, XPM and FWM contributions to the overall NLIN in a  $30 \times 100$ -km system with 115 channels using QPSK, 16-QAM where, overall NLIN (black) and its SPM (green), XPM (blue) and FWM (red) components respectively. There are three types of nonlinear effects contributions on a subcarrier level which includes SPM, XPM and FWM etc. The contribution only on interested subcarriers where distortions generated thereby nonlinear interactions involved which is referred as SPM. Similarly, contributions are generated by nonlinear interactions between the subcarrier of interest and a single interfering subcarrier, which is known as XPM. Whereas, two or three interfering subcarriers are involved, then, it is referred as FWM. It is most significant nonlinear effect among others due to the huge contribution of the number of increased subcarriers. This can be explained with the help of frequency-domain picture of NLIN in which the number of subcarriers increases, their bandwidth becomes narrower and more NLIN products involve frequency tones from three different subcarriers. On the whole, both XPM and FWM distortions constitute important NLIN contributions for an optimal number of subcarriers given by the minimum overall NLIN. It is clearly indicated that FWM is mainly independent of the modulation format, while XPM and SPM show pronounced format dependence. To better understand the modulation format dependence of XPM and its scaling with the number of subcarriers, use the time-domain pulse-collision theory to separate XPM contributions into 2-pulse collisions (inducing PPRN only) as opposed to 3- and 4-pulse collisions (inducing PPRN plus higher-order ISI terms). Hence, these individual XPM for different modulation formats, with 2-pulse collisions exhibiting strong modulation format dependence and 3-

and 4-pulse collisions being mostly format independent. While the 3- and 4-pulse contributions monotonically decrease with the number of subcarriers, the 2-pulse contributions exhibit a concave dependence with the number of subcarriers. This is because the temporal width of the transmitted pulses increases with the number of subcarriers.

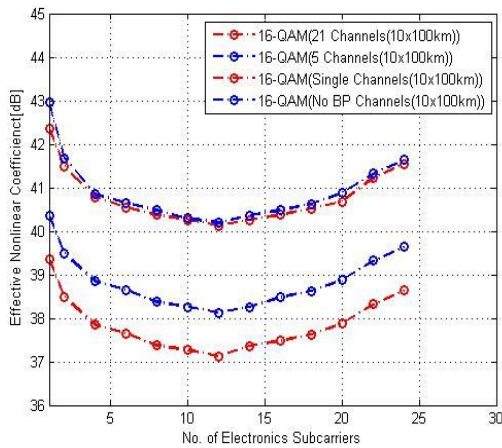


Fig. 10 Effective nonlinear coefficient as a function of the number of subcarriers  $M$  in 21-channel systems with and without BP.

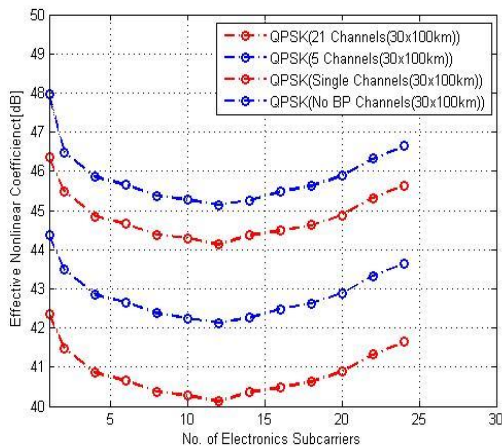


Fig. 11 Number of optical channels that are back-propagated (for example, 3-channel BP assumes the joint BP of  $3M$  subcarriers).

As the pulses become wider, the impact of dispersion on the individual subcarriers is less significant and the number of pulses that overlap during propagation decreases. Consequently, the number and significance of 3- and 4-pulse collisions quickly decreases (recall that 3- and 4-pulse collisions involve two overlapping pulses from the same subcarrier) while 2-pulse collisions become increasingly important. For a sufficiently large number of subcarriers 2-pulse collisions become less important again as the width of the pulses is relatively large with respect to the length of the link and collisions tend to be more incomplete. In this regime, FWM contributions accumulate along the link more efficiently as phase-matching conditions become better fulfilled.

### C. Systems without nonlinear PPRN mitigation:

Next to investigate the dependence of NLIN on the number of subcarriers in systems employing digital BP. Figure 18 shows the effective nonlinear coefficient as a function of  $M$  in 21-channel systems. Lines represent theoretical predictions and markers correspond to split-step simulations for systems without BP and with perfect single-, 3- and 5-channel BP, performed. Note that the number of back-propagated channels refers to the number of back-propagated optically modulated channels (for example, single channel BP assumes that all  $M$  subcarriers of the individual channels are jointly back-propagated). Theory and simulations agree to within 0.35 dB. In Fig. 10 and 11 shows that the dependence of the NLIN on the number of subcarriers and the optimal  $M$  which minimizes the effective nonlinear coefficient do not differ significantly between systems with and without BP.

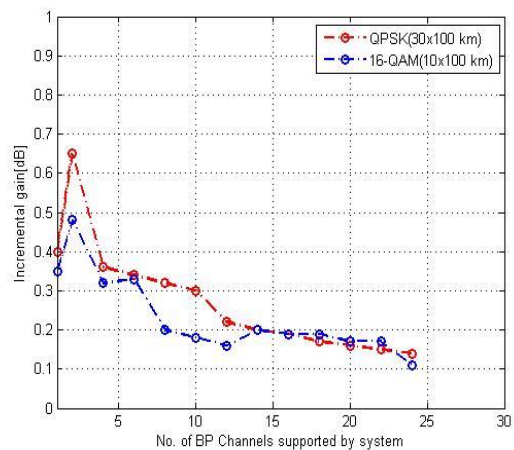


Fig. 12 Additional peak-SNR gain obtained from increasing the number of back-propagated channels from  $(N - 2)$  to  $N$ , with  $N$  being odd.

From the plot the peak-SNR gain of BP as a function of the number of spans in fully loaded systems with 115 channels. The subcarrier-multiplexed transmission carried by the number of subcarriers is optimized separately for each case. In contrast to systems without SCM, we consider only the BP of an odd number of channels since only in these cases our subcarrier of interest (which is the center subcarrier of the center channel) is in fact the center subcarrier within the group of jointly back-propagated channels. When an even number of channels are jointly back-propagated our subcarrier under test exhibits a smaller BP gain than the true center subcarrier, cf. Fig. 12. This is why in Fig. 19c we also only show the incremental gain resulting from increasing the number of back-propagated channels from  $N-2$  to  $N$ , with  $N$  being odd. That is, the presented incremental gains are per back-propagated channel pair, in contrast to the respective single-carrier curves. The benefit of single-, 3- and 5-channel BP is shown to be limited to about 0.4 dB, 1 dB, and 1.3 dB for systems using QPSK and 0.4 dB, 0.9 dB, and 1.2 dB for systems



using high-order QAM formats. The additional gain provided by increasing the number of jointly back-propagated channels beyond five is limited to about 0.2 dB per pair of additional jointly back-propagated channels. Comparing these results with the results of Fig. 10 reveals that the gains of BP in systems with SCM do not differ significantly from their value in systems without SCM, which makes the gains from SCM and the gains from BP additive in a systems context.

## V. CONCLUSION

In this paper, two key NLC strategies have been discussed to limit the in-band and out-of-band nonlinearity in massively loaded WDM systems. The nonlinear processing capability of the multi-channel optical carriers as well as subcarrier multiplexed systems at various spectral efficiencies, operating both in point-to-point and in optically routed networking contexts were investigated. The NLIN contributions are calculated with the help of a freely available on-line tool (the NLIN Wizard). According to this, the peak SNR gains at the optimum launch power for ideal multi-channel BP and ideal PPRN removal for both single-carrier and electronically subcarrier multiplexed optical modulation have been summarized in Table. IV. The BP of single-/3-/5-channel result conveys that the peak SNR gain increased for each additional jointly back-propagated channel (i.e. SCM systems gives half of the incremental gain for each pair of back-propagated channels). The potential peak-SNR gain of BP saturates quickly with the joint BP processing bandwidth which is given in the single-carrier systems (first results column in Table. II). In the case of 3,000-km QPSK system, it is found that the peak SNR gain around 0.5/0.9/1.2 dB for 1/3/5-channel BP along with less than 0.1 dB of additional gain per further co-processed channel. The PPRN removal for QPSK has taken a gain potential of 0.2 dB.

On the whole, the combination with multi-channel BP gives a total in-band plus out-of-band gain potential of 0.8/1.3/1.6 dB for single-/3-/5-channel BP. Based on this, even 3-channel BP is beyond the capability as compared with coherent ASICs, where three 32-Gbaud channels are required for nonlinear co-processing. Therefore, 16-/64-/256-QAM systems have a similar gain potential as for QPSK under multi-channel BP, which shrinks link shorter considerably as the higher-order QAM formats due to their inherently reduced noise tolerance and their increased implementation penalties, this gain reduction for QAM is practically relevant. That is, the gain of BP is limited to no more than 0.2/0.6/0.8 dB for single-/3-/5-channel BP for 100-km links. However, the gain potential of PPRN removal is dramatically increased for QAM, especially as the link gets shorter. Similarly, the combination with multi-channel BP gives a total in-band plus out-of-band gain potential of 4.3/5.6/6.3 dB for single-/3-/5-channel BP.

The huge gain potential can be practically exhausted depends effective PPRN removal algorithms operated which will be able to mitigate PPRN, whose temporal correlations are significantly reduced for shorter links. (For example, while PPRN is correlated over around 100 symbols for  $10 \times 100$ -km links, the correlation is reduced to only about 10 symbols for a single 100-km link). With the help of SCM, the peak SNR gain is obtained around 0.8 dB along with optimal subcarrier 12 has required for further co-processed channel for 3,000 km QPSK system. Due to this gain has reduced substantially for higher-order QAM, and especially when going to shorter link lengths, where the optimum number of subcarrier steadily shrinks, until single-carrier systems become optimum for single-span links. Therefore, adding BP to a SCM system has found a similar peak SNR gain for single-carrier systems, such as 0.4/1.0/1.3 dB for single-/3-/5-channel BP, again saturated limited less than 0.1 dB of gain per additionally jointly back-propagated optical channel. As compared with BP, the combination of BP with SCM produced an effective result such as 1.2/1.8/2.1 dB for 1-/3-/5-channel BP compared to a single-carrier system without BP. The QPSK transmission over  $30 \times 100$  km enjoys a potential gain of 0.7 dB at the optimum subcarrier count (instead of 0.2 dB in single-carrier systems), in addition to the 0.8 dB of gain resulting from the use of SCM, whereas QAM transmission over  $10 \times 100$  km enjoys a 1.4 dB potential gain (instead of 0.7 dB), in addition to the 0.3 dB SCM gain. These results imply that SCM can be advantageous not only for constant modulus formats but also for high spectral efficiency systems employing nonlinear PPRN mitigation. As the correlation of PPRN (in terms of symbols per subcarrier) shrinks with the number of subcarriers per channel, joint subcarrier processing may have to be used to re-establish correlations and compensate PPRN as effectively as in single-carrier systems. In addition, employing both BP and PPRN removal can yield better results than what is found in the equivalent single-carrier system. For example, while single-carrier QAM over  $10 \times 100$  km has a gain potential of 1.4/2.0/2.3 dB for single-/3-/5-channel BP in combination with PPRN removal, the equivalent SCM system, with an optimum of 7 subcarriers per optical channel, may show up to 1.9/2.9/3.6 dB of gain, in addition to 0.3 dB of gain from SCM. In addition and most importantly, the benefit of BP with digital SCM context is not only in improving system robustness to nonlinearities but also in decreasing the performance variations in various network scenarios. These variations were shown to be substantial for single-carrier systems, but indistinguishably small for SCM systems with a sufficiently large number of subcarriers. Future schemes could provide higher gains than predicted here if they could suppress the impact of out-of-band higher-order XPM terms and FWM contributions that are currently assumed to be non-removable distortions.

TABLE II Potential peak-SNR gains in fully-loaded WDM systems

| Modulation format                            | NLIN compensation technique | Single-carrier                       | Electronic subcarrier multiplexing |                                     |
|--|-----------------------------|--------------------------------------|------------------------------------|-------------------------------------|
| QPSK<br>50 × 100 km                          | Digital BP                  | 0.5/0.9/1.2 dB<br>+ <0.1 dB per ch.  |                                    | 0.4/1.0/1.3 dB<br>+ <0.1 dB per ch. |
|  | PPRN removal                | 0.2 dB                               | 0.8 dB<br>15 subcarriers           | 0.6 dB                              |
|  | BP and PPRN removal         | 0.8/1.2/1.5 dB<br>+ <0.1 dB per ch.  |                                    | 0.9/1.7/2.2 dB<br>+ <0.2 dB per ch. |
| QPSK<br>30 × 100 km                          | Digital BP                  | 0.5/0.9/1.2 dB<br>+ <0.1 dB per ch.  |                                    | 0.4/1.0/1.3 dB<br>+ <0.1 dB per ch. |
|  | PPRN removal                | 0.2 dB                               | 0.8 dB<br>15 subcarriers           | 0.7 dB                              |
|  | BP and PPRN removal         | 0.8/1.3/1.6 dB<br>+ <0.1 dB per ch.  |                                    | 1.1/1.9/2.7 dB<br>+ <0.2 dB per ch. |
| High-order QAM<br>(16,64,256)<br>10 × 100 km | Digital BP                  | 0.4/0.8/1.1 dB<br>+ <0.1 dB per ch.  |                                    | 0.4/0.8/1.1 dB<br>+ <0.1 dB per ch. |
|  | PPRN removal                | 0.7 dB                               | 0.3 dB<br>7 subcarriers            | 1.4 dB                              |
|  | BP and PPRN removal         | 1.4/2.0/2.3 dB<br>+ <0.15 dB per ch. |                                    | 1.9/2.9/3.6 dB<br>+ <0.2 dB per ch. |
| High-order QAM<br>(16,64,256)<br>5 × 100 km  | Digital BP                  | 0.3/0.8/1.0 dB<br>+ <0.1 dB per ch.  |                                    | 0.3/0.8/1.0 dB<br>+ <0.1 dB per ch. |
|  | PPRN removal                | 0.9 dB                               | 0.2 dB<br>5 subcarriers            | 1.6 dB                              |
|  | BP and PPRN removal         | 1.6/2.4/2.9 dB<br>+ <0.15 dB per ch. |                                    | 2.2/3.3/4.0 dB<br>+ <0.2 dB per ch. |
| High-order QAM<br>(16,64,256)<br>1 × 100 km  | Digital BP                  | 0.2/0.6/0.8 dB<br>+ <0.1 dB per ch.  |                                    | 0.2/0.6/0.8 dB<br>+ <0.1 dB per ch. |
|  | PPRN removal                | 2.5 dB                               | 0 dB<br>Single-carrier             | 2.5 dB                              |
|  | BP and PPRN removal         | 4.3/5.6/6.3 dB<br>+ <0.2 dB per ch.  |                                    | 4.3/5.6/6.3 dB<br>+ <0.2 dB per ch. |

## References

- [1] A. R. Chraplyvy, "Limitations on lightwave communications imposed by optical-fiber nonlinearities," *J. Lightwave Technology*, vol. 8, pp.1548–1557 (1990).
- [2] G. P. Agrawal, *Nonlinear Fiber Optics*, Academic press (2007).
- [3] E. Ip and J. M. Kahn, "Compensation of dispersion and nonlinear impairments using digital backpropagation," *J. Lightwave Technology*, vol. 26, pp. 3416–3425 (2008).
- [4] M. Secondini and E. Forestieri, "On XPM mitigation in WDM fiberoptic systems," *IEEE Photon. Technol. Lett.*, vol. 26, pp. 2252–2255 (2014).
- [5] R. Dar, M. Feder, A. Mecozzi, and M. Shtaif, "Inter-channel nonlinear interference noise in WDM systems: Modeling and mitigation," *J. Lightwave Technology*, vol. 33, pp. 1044–1053 (2015).
- [6] S. Chandrasekhar, X. Liu, B. Zhu, and D. W. Peckham, "Transmission of a 1.2-Tb/s 24-carrier no-guard-interval coherent OFDM superchannel over 7200-km of ultra-large-area fiber," *European Conference on Optical Communication (ECOC)*, paper PD2.6 (2009).
- [7] G. Bosco, V. Curri, A. Carena, P. Poggiolini, and F. Forghieri, "On the performance of Nyquist-WDM terabit superchannels based on PMBPSK, PM-QPSK, PM-8QAM or PM-16QAM subcarriers," *J. Lightwave Technology*, vol. 29, pp. 53–61 (2011).
- [8] S. Chandrasekhar and X. Liu, "OFDM based superchannel transmission technology," *J. lightwave technology*, vol. 30, pp. 3816–3823 (2012).
- [9] E. Temprana, E. Myslivets, B. P. Kuo, L. Liu, V. Ataie, N. Alic, and S. Radic, "Overcoming Kerr-induced capacity limit in optical fiber transmission," *Science*, vol. 348, pp. 1445–1448 (2015).
- [10] P. Poggiolini, A. Nespola, Y. Jiang, G. Bosco, A. Carena, L. Bertignono, S. M. Bilal, S. Abrate, and F. Forghieri, "Analytical and experimental results on system maximum reach increase through symbol rate optimization," *J. Lightwave Technology*, vol. 34, pp. 1872–1885 (2016).
- [11] D. Marsella, M. Secondini, E. Agrell, and F. Forestieri, "A simple strategy for mitigating XPM in nonlinear WDM optical systems," *Optical Fiber Communication Conference (OFC)*, paper Th4D-3 (2015).

- [12] Y. Tang, W. Shieh, and B. S. Krongold, "DFT-spread OFDM for fiber nonlinearity mitigation," *IEEE Photonics Technology Letters*, vol. 22, pp. 1250-1252 (2010).
- [13] L. B. Du and A. J. Lowery, "Optimizing the subcarrier granularity of coherent optical communications systems," *Optics Express*, vol. 19, pp.8079-8084 (2011).
- [14] A. Bononi, N. Rossi, and P. Serena, "Performance dependence on channel baud-rate of coherent single-carrier WDM systems," *European Conference on Optical Communication (ECOC)*, paper Th.1.D.5 (2013).
- [15] M. Qiu, Q. Zhuge, M. Chagnon, Y. Gao, X. Xu, M. Morsy-Osman, and D. V. Plant, "Digital subcarrier multiplexing for fiber nonlinearity mitigation in coherent optical communication systems," *Optics Express*, vol. 22, pp. 18770-18777 (2014).
- [16] R.-J. Essiambre, G. Kramer, P.J. Winzer, G.J. Foschini, and B. Goebel, "Capacity limits of optical fiber networks," *J. Lightwave Technology*, vol. 28, pp. 662-701 (2010).
- [17] P. Serena, "Nonlinear signalnoise interaction in optical links with nonlinear equalization," *J. Lightwave Technology*, vol. 34, pp. 1476- 1483 (2016).
- [18] N. V. Irukulapati, H. Wymeersch, P. Johannisson, and E. Agrell, "Stochastic digital backpropagation," *IEEE Transaction on Communication*, vol. 62, pp. 3956-3968 (2014).
- [19] D. Rafique and A. D. Ellis, "Impact of signal-ASE four-wave mixing on the effectiveness of digital backpropagation in 112 Gb/s PM-QPSK systems," *Optics Express*, vol. 19, pp. 3449-3454 (2011).
- [20] R.-J. Essiambre and P. J. Winzer, "Fibre nonlinearities in electronically pre-distorted transmission," *European Conference on Optical Communication (ECOC)*, paper Tu.3.2.2 (2005).
- [21] X. Li, X. Chen, G. Goldfarb, E. Mateo, I. Kim, F. Yaman, and G. Li, "Electronic post-compensation of WDM transmission impairments using coherent detection and digital signal processing," *Optics Express*, vol. 16, pp. 880-888 (2008).
- [22] W. Yan, Z. Tao, L. Dou, L. Li, S. Oda, T. Tanimura, T. Hoshida, and J. C. Rasmussen, "Low complexity digital perturbation back-propagation," *European Conference on Optical Communication (ECOC)*, paper Tu-3 (2011).
- [23] A. Ghazisaeidi and R.-J. Essiambre, "Calculation of coefficients of perturbative nonlinear pre-compensation for Nyquist pulses," *European Conference on Optical Communication (ECOC)*, paper WE.1.3.3 (2014).
- [24] F. P. Guiomar, J. D. Reis, A. L. Teixeira, and A. N. Pinto, "Mitigation of intra-channel nonlinearities using a frequency-domain Volterra series equalizer," *Optics Express*, vol. 20, pp. 1360-1369 (2012).
- [25] E. F. Mateo, L. Zhou, and G. Li, "Impact of XPM and FWM on the digital implementation of impairment compensation for WDM transmission using backward propagation," *Optics Express*, vol. 16, pp. 16124-16137 (2008).
- [26] D. S. Millar, S. Makovejis, C. Behrens, S. Hellerbrand, R. I. Killely, P. Bayvel and S. J. Savory, "Mitigation of fiber nonlinearity using a digital coherent receiver," *J. Selected Topics in Quantum Electronics*, vol. 16, pp. 1217-1226 (2010).
- [27] D. Rafique, M. Mussolin, M. Forzati, J. M'artensson, M. N. Chughtai, and A. D. Ellis, "Compensation of intra-channel nonlinear fibre impairments using simplified digital backpropagation algorithm," *Optics Express*, vol. 19, pp. 9453-9460 (2011).
- [28] L. B. Du and A. J. Lowery, "Improved single channel backpropagation for intra-channel fiber nonlinearity compensation in long-haul optical communication systems," *Optics Express*, vol. 18, pp. 17075-17088 (2010).
- [29] Z. Tao, L. Dou, W. Yan, L. Li, T. Hoshida, and J. C. Rasmussen, "Multiplier-free intrachannel nonlinearity compensating algorithm operating at symbol rate," *J. Lightwave Technology*, vol. 29, pp. 2570-2576 (2011).
- [30] M. Secondini, D. Marsella, and E. Forestieri, "Enhanced split-step Fourier method for digital backpropagation," *European Conference on Optical Communication (ECOC)*, paper We.3.3.5 (2014).